

Airway Tree Segmentation By Removing Paths of Leakage

Gang Song¹, Nicholas Tustison¹, James C. Gee¹,

Penn Image Computing and Science Laboratory (PICS), Dept. of Radiology,
University of Pennsylvania, Philadelphia, PA, USA,

Abstract. This paper describes a new method for airway segmentation from CT images. We propose a form of adjusted image gradients for thin airways segmentation and apply it in multi-stencil fast marching. A graph of airway path segments is constructed from the arrival time function of fast marching. Instead of detecting leakage during segmentation, our method verifies each path segment in a separate step, using a novel leakage cost function defined on the whole path. Our scheme of path removal can be viewed as complementary post-processing for existing region growing methods. Experiments show that the proposed method can remove leakage regions while keeping most thin airways.

1 Introduction

Segmentation of airway trees from computed tomography images is critical for various clinical applications involving pulmonary diseases. Diameters of fourth generation airway in a typical CT image are about two or three voxels wide. The limitation of imaging resolution and noise lead to the inhomogeneity of image intensities inside airway walls and also the blurring effects around airway walls. These factors make the balance between detecting leakage and extending thin airways very critical in airway segmentation

Various algorithms have been proposed in the literature. Schlathölter et al used level set methods for a simultaneous segmentation and tree reconstruction framework [1]. The authors proposed several heuristic rules to detect leakage in the growing regions. Tschirren et al proposed to keep an active region of cylinder shape [2]. By tracking the orientation of active cylinder, the active region was extended to next possible airway location. A multi-threshold approach was adopted in [3] to increase robustness in growing airways trees. Recent work from Christian et al [4] used gradient vector flow to guide growing direction. The work of [5] focused on extending thin airways by computing the shortest paths inside a search sphere from end points in the initial segmentation.

Many of these algorithms have shown successful segmentation of the bronchi and trachea. However, for the third and higher generations in the airway tree, current segmentation results still have room for improvement, indicated by a recent evaluation on 15 airway segmentation algorithms [6].

In this paper we explore a new approach in airway segmentation. Instead of mixing airway segmentation and leakage detection at every iteration as in

[4, 5], we divide this problem into a hypothesis generation of thin airway paths and a post processing procedure of removing leakage path candidates. For the purpose of generating as many hypotheses as possible, we propose a novel speed function for thin airways. To exclude leakage regions, we propose a novel cost function defined on the whole path candidate. Such a scheme is more flexible when evaluating the whole path and can be viewed as complementary to current region growing methods.

2 Methods

Our method includes two steps: path candidate generation and path candidate removal. In the first step, we generate all initial path candidates in the segmentation using the fast marching method. A new formulation of adjusted image gradients is proposed to compute the speed image. Path candidates are then extracted by back tracing in the arrival time function. Next, those paths which may contain the leakage regions are further removed from the initial segmentation using our novel leakage cost function.

2.1 Initial Segmentation Using Speed Function on Adjusted Gradients

We use fast marching as the first step to generate the initial airway segmentation. The arrival time is modeled by the Eikonal equation $|\nabla T|F = 1$, where F is the speed function of the propagation front and T is the arrival time. Given the 3D image volume I , one form of the gradient based speed function is $F = e^{-\beta|\nabla I|}$ used in [1]; β is a scalar weighting coefficient.

By definition ∇I usually has high values at the locations close to the boundary of airways, both inside and outside the airway. Thus fast marching will have a low speed along the boundary inside airways. For the trachea and bronchi, this is not a practical problem since the airway boundary takes a small portion in the whole volume. However, for thin airways (like fourth order airways), where the diameter of the airway is about two voxels wide, the speed F would be low along whole thin airway segment and this would prevent fast marching from successfully extending further (See Fig. 1b).

Using $|\nabla I|$ directly is not suitable for front propagation along thin airways with partial volume effect. One way to deal with this problem is to interpolate image to a higher resolution, or to assign a special label for airway boundaries in fast marching. Here we propose a different solution by adjusting the definition of image gradients. The ideal gradient for airway segmentation should be defined only on the wall of airways (brighter voxels) rather than inside airways (darker voxels), such that the speed inside airways are high while low outside. To formalize this notion, the following modified gradient is proposed:

$$g(x) = \begin{cases} |\nabla I(x)| & \text{if } |I(x + \frac{1}{2}\mathbf{n}_x) - I(x)| < |I(x) - I(x - \frac{1}{2}\mathbf{n}_x)|; \\ 0 & \text{otherwise.} \end{cases} \quad (1)$$

\mathbf{n}_x is the unit direction of the gradient: $\mathbf{n}_x = \frac{\nabla I(x)}{|\nabla I(x)|}$ and is measured in voxel units. Note that this definition is not for leakage detection, but for generating all possible airway segmentation.

With this gradient definition, the corresponding front propagation equation becomes $F = e^{-\beta g(x)}$. A seed point x_0 in the trachea region is selected as the initial condition $T(x_0) = 0$. A comparison of results using $g(x)$ and $|\nabla I(x)|$ is shown in Fig.1. The fast marching gives the correct segmentation using the proposed $g(x)$ on this thin airway segment.

Another issue in solving front propagation for thin airways is the choice of connectivities. Many airway segments are extended along diagonal directions. However, Sethian's original fast marching method (FMM, [7]) is not accurate along these directions as it computes the derivative using 6-connectivity. In order to adopt the 26-connectivity in fast marching, we applied the multi-stencil fast marching method (MSFM, [8]) to solve the equation in practice. Compared to FMM, MSFM solves the equation along several predefined stencils to cover the entire 26 neighboring locations. For those stencils that are not aligned with the natural coordinate system, the equation is derived using directional derivatives. Details of MSFM can be found in [8]. A 26-connectivity is especially important for fast marching in thin airways when one location has no 6-connectivity neighbors in the airway.

2.2 Path Candidate Generation from Initial Segmentation

Given the arrival time function T and a threshold t_0 , the initial segmentation is obtained as $S = \{x | T(x) < t_0\}$. S contains both airway tree segments and leakage regions. A nice property of the function T is that the propagation path from any given location to the seed location x_0 can be traced back using the gradient of T . Our motivation is to cluster voxels in S into different path segments. In

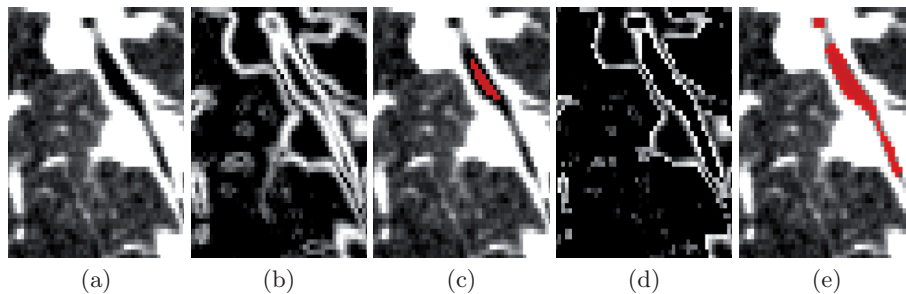


Fig. 1. Example of the proposed adjusted image gradients. (a) A region containing a thin airway (b) Gradients computed as $|\nabla I|$. Note that it has high gradients inside the airway, which prevent fast marching. (c) Airway segmentation using (b) to compute speed image and MSFM. (d) Adjusted gradients computed using $g(x)$. Only the gradients in the bright airway wall are preserved. (e) Airway segmentation using adjusted gradients in (d) to compute speed image and MSFM.

turn, leakage can be detected on voxels in each path segment as a whole, instead of on each voxel individually.

More formally, a graph G is built to describe the structure of the binary mask S . Each node in G is a cluster of voxels in S , corresponding to part of the airway or to part of the leakage. We apply an approach similar to [1] and [9] to get the graph G .

First a distance field, $D(x)$, to the initial seed point x_0 is computed in the domain S . Then each continuous value $D(x)$ is discretized into an integer j such that $D_0(x) = j$ if $jh \leq D(x) < (j+1)h$, in which h is the bin width for discretization. By assigning a node n to one connected component of the same integer value in $D_0(x)$, a graph G is constructed from S . Neighboring connected components are connected in the graph. The bin width h controls the shape of each node in the airways so that a node is roughly a tube-like structure. An example of the graph construction using discretization is illustrated in Fig.2.

The propagation from initial seed point x_0 to a voxel x_1 in S , denoted as $C_{x_0}^{x_1}$, can be traced by solving ordinary differential equation $\frac{dC(t)}{dt} = -\frac{\nabla D}{|\nabla D|}$ with boundary condition $C(t_1) = x_1$ and $C(0) = x_0$. We define the path from x_0 to x_1 on the graph G as the series of nodes that intersect with $C(t)$:

$$P_{x_0}^{x_1} = \{n | n \in G, n \cap C_{x_0}^{x_1} \neq \emptyset\} \quad (2)$$

2.3 Leakage Removal Using Cost Function on Path Nodes

Each path segment node n in G is a candidate for leakage removal. We consider three properties of the path segment: its volume, its vesselness measurement and how it is separated from the background in the image. The first two properties

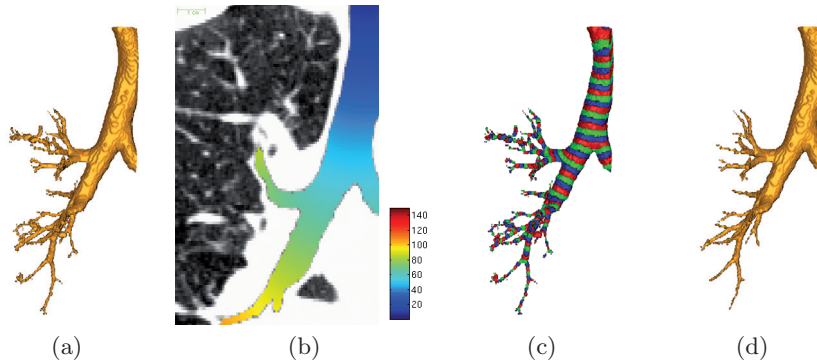


Fig. 2. Path graph construction. Only the airway tree in the right lung is shown. (a) Initial segmentation S using fast marching with adjusted gradients. (b) Distance transform D inside S with color bar shown on the right. (c) Graph G using discretization on D . Nodes $\{n\}$ are colored by red, green and blue. Each node n has the same discretization value in D_0 and belong to the same connected component. (d) Final segmentation of airway tree using our path segment removal approach.

have been investigated in the literature [1, 4, 5]. In this paper we use Frangi's vesselness definition [10] on dark tubes to measure each voxel in n . Those voxels of vesselness smaller than t_{vessel} are removed from node n . The nodes of a volume greater than a threshold t_{vol} are also removed. These two properties make sure that path segment n is of a tube-like shape, however, it may still contain leakage areas (see Fig.3 for an example).

We propose a novel leakage cost function to estimate how each path node can be separated from background. For each node n , its medial axis is computed as the segment direction \cdot . The local coordinate system use this direction as z axis of the segment. The surrounding region of n (obtained from image dilation operation) is then divided into k sections by different angles uniformly distributed in the x - y plane. Fig.3 shows an example of $k = 8$ sections in different colors. If the node has leaked into the background from some direction, the average gradient in that section would be low.

The leakage cost on path n , $S(n)$, is defined as the minimum of average gradients in all sections:

$$S(n) = \min_i \frac{1}{|N_i(n)|} \sum_{x \in N_i(n)} g(x) \quad (3)$$

where $g(x)$ is the adjusted gradient in section 2.1, $N_i(n)$ is the neighborhood of n in the i -th angle. The nodes of $S(n)$ lower than a threshold t_{path} are considered as leakage and are removed from G . The final airway segmentation is the connected component in G that contains most remaining nodes.

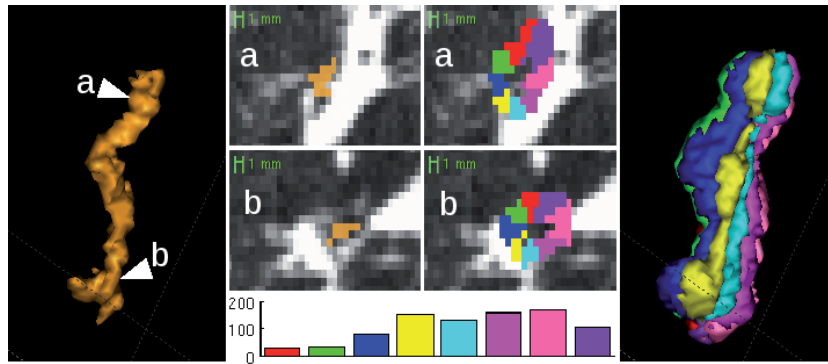


Fig. 3. Example of the proposed path leakage cost function on a node of leakage. *Left:* shape of the node is similar to airway, but is not part of airway. *First and second rows in the middle:* on left) one 2D slice with the path n shown in brown; on right) $k = 8$ sections of the neighborhood of n in different directions, each section $N_i(n)$ shown in different colors. *Last row in the middle:* bar plots of $\frac{1}{|N_i(n)|} \sum_{x \in N_i(n)} g(x)$ with each i shown in corresponding colors. *Right:* surface rendering of the $k = 8$ sections. Location a has an leakage in the upward direction; however location b is difficult to segment locally. Our proposed cost $S(n)$ is defined as the minimum of the $k = 8$ values (the red bar here), which is significantly lower than other bars.

3 Results

The proposed method was applied to extract airways in four canine specimens at 15 months after pulmonary lobe surgery (part of lobes were removed). The images were taken under forced inflationary pressure of 30 cm H₂O. All images have a slice thickness of 1.25 mm and in-plane resolution of 0.46×0.46 mm². The airways in these volumes were semi-supervised extracted and manually modified as the ground truth for evaluation.

In all our experiments, parameter β used in computing speed function was set to 0.05. The initial segmentation threshold t was 200. The distance field $D(x)$ was discretized by bin width $h = 2$. The value of h is related to the length of the node in practice. We tested h from 2 to 4 and got similar results.. We applied the multi-scale strategy when computing Frangi's vesselness, using four scales $s = 0.5, 1, 2, 3$ (see the discussion of scale s in [10]). For each path node n , its surrounding neighborhood was obtained by computing the dilation of radius= 3 and was further divided to $k = 8$ sections along the segment direction. The vesselness threshold was 30 and the volume threshold was 1000. The final segmentation was given by removing all path nodes whose path leakage cost $S(n)$ was lower than 10.

Our method requires a seed point in the trachea region as the initial condition for fast marching. While such points could be easily manually selected, we further automated the whole process by applying Hough transform on circles. Assuming that the trachea was roughly aligned with z axis in image volume, we scanned each slice along z axis from the top and the seed point x_0 was identified as the center of the first detected circle.

All final segmentation results S were evaluated against the manually labeled airway trees S_g . Using $|\cdot|$ to denote the number of voxels in a set, we computed the recall rate as $\frac{|S \cup S_g|}{|S|}$, the false alarm rate as $\frac{|S - S_g|}{|S|}$ and the missing rate as $\frac{|S_g - S|}{|S_g|}$. As trachea and bronchi are relatively easy to segment using region growing approaches and our main interest was to extract thin airways, these regions were excluded in computing both S and S_g . Another reason is that the trachea and bronchi might take up to 95% volume in the whole airways; thus it should be excluded as a huge bias in evaluating thin airways. An example of our final segmentation is illustrated in Fig.4. Missing regions $S_g - S$ are colored in blue and false alarm regions $S - S_g$ in red (in Fig.4b).

On the four canine specimens, our algorithm got the average recall rate of 96.8% and the missing rate is 8.2%. Most missing regions are extended from the end segments of 2 to 3 voxels wide. The false alarm rate is 3.2%, but we observed that many of the false alarm regions are due to the human label errors. These are not leakage regions in segmentation, which shows the good performance of our path elimination approach in preventing leakage while keeping most airways.

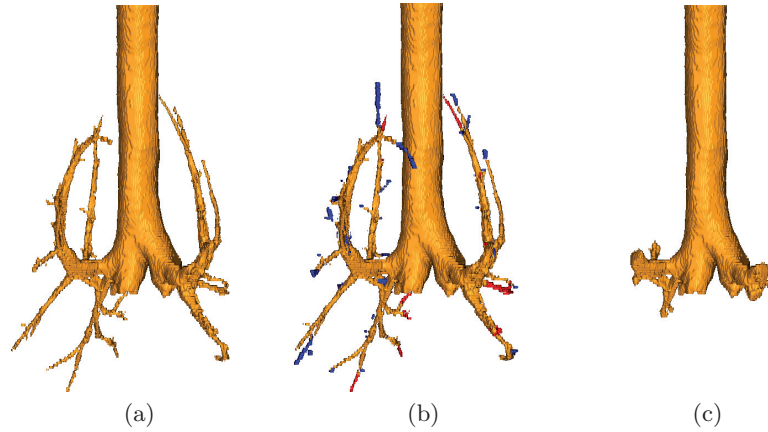


Fig. 4. Surface rendering of an example result using the proposed method. (a) Segmented airways using our approach. (b) Comparison with ground truth. The blue regions are labeled in ground truth but missing in our results. The red regions are labeled in our results but missing in ground truth. The brown regions exist in both ground truth and our results. (c) Example of the trachea and bronchi region, which is excluded when computing the rates.

4 Discussion

In this paper we proposed a new method for extracting airway trees from 3D computed tomography images. We focused our method on removing leakage regions while still segmenting most thin airways. Compared to existing region growing methods, our method has a unique path removal procedure to exclude potential leakage. A graph of path candidates is constructed from the arrival time using the fast marching method. The leakage regions are identified from all path segment candidates using our proposed leakage cost function. A similar idea of checking different directions was proposed in [11]. They used gradients in different radial directions from one voxel to track vessels. In comparison, our cost function is defined on the node of a whole path segment for leakage removal. Each node is a higher level structure, which is more robust to noise and has a more flexible definition. Furthermore, this is not a linear measurement which means it can not be represented as an integration along the path. Thus we do not use Dijkstra’s algorithm, which was used in [5].

The second contribution in this paper is that we proposed a form of adjusted gradient in computing speed image. We also apply multi-stencil fast marching for a 26 connectivity neighborhood in thin airway segmentation. We show that thin airways of 2 to 3 voxels wide can be extracted by our adjusted image gradients and utilizing the connectivities along diagonal directions in fast marching.

It should be noted that our approach is not contradictory to existing region growing methods. By separating the leakage detection as a post processing step, our method can take the advantage of current work on region growing while

reducing leakage. The result from one approach can be used as input to the other. For example, the missing rate in our experiment may be further improved using the method in [5] in the stage of generating path candidates.

The number of datasets used in the evaluation is limited. A larger evaluation data set is needed in our future work. Also, we used manual segmentation as our ground truth. An alternative for constructing the reference is combining results from different algorithms as in [6]. It would also be interesting to test our algorithm on the output of other algorithms to verify the effectiveness of post-processing.

References

1. Schlathölder, T., Lorenz, C., Carlsen, I., Renisch, S., Deschamps, T.: Simultaneous segmentation and tree reconstruction of the airways for virtual bronchoscopy. In: SPIE International Symposium on Medical Imaging. (2002) 103–113
2. Tschirren, J., Hoffman, E., McLennan, G., Sonka, M.: Intrathoracic airway trees: segmentation and airway morphology analysis from low-dose ct scans. *Medical Imaging, IEEE Transactions on* **24**(12) (dec. 2005) 1529–1539
3. van Ginneken, B., Baggerman, W., van Rikxoort, E.: Robust segmentation and anatomical labeling of the airway tree from thoracic ct scans. In: *Medical Image Computing and Computer-Assisted Intervention*. (2008) 219–226
4. Bauer, C., Bischof, H., Beichel, R.: Segmentation of airways based on gradient vector flow. In: *The Second International Workshop on Pulmonary Image Analysis*. (2009) 191–201
5. Lo, P., Sporning, J., Pedersen, J.J., Bruijne, M.: Airway tree extraction with locally optimal paths. In: *Medical Image Computing and Computer-Assisted Intervention*. (2009) 51–58
6. Lo, P., van Ginneken, B., Reinhardt, J., de Bruijne, M.: Extraction of airways from ct (exact’09). In: *Second International Workshop on Pulmonary Image Analysis*. (2009) 175–189
7. Sethian, J.A.: *Level Set Methods and Fast Marching Methods: Evolving Interfaces in Computational Geometry, Fluid Mechanics, Computer Vision, and Materials Science*. 2 edn. Cambridge University Press (June 1999)
8. Hassouna, M.S., Farag, A.A.: Multistencils fast marching methods: A highly accurate solution to the eikonal equation on cartesian domains. *IEEE Transactions on Pattern Analysis and Machine Intelligence* **29** (2007) 1563–1574
9. Hassouna, M.S., Farag, A.A.: Robust centerline extraction framework using level sets. In: *Computer Vision and Pattern Recognition (CVPR’05)*. (2005) 458–465
10. Frangi, A.F., Niessen, W.J., Vincken, K.L., Viergever, M.A.: Multiscale vessel enhancement filtering. In: *Medical Image Computing and Computer-Assisted Intervention*. (1998) 130–137
11. Wink, O., Niessen, W., Viergever, M.: Fast delineation and visualization of vessels in 3-d angiographic images. *IEEE Transactions on Medical Imaging*, **19**(4) (april 2000) 337–346